Data
Models
Inventories

PARIS

Process Attribution of Regional Emissions

GA 101081430, RIA

Inverse estimates of fossil fuel CO_2 emission

Disclaimer: *The results presented in this report are highly preliminary, and are intended to show the current state of the model development being undertaken in PARIS. We do not recommend that these results be used outside of the PARIS project without first discussing their limitations with the report authors. Further developments that build on these preliminary results will be published in a timely manner by the PARIS team.*

Milestone M24			
Delivery due date Annex I	PM 16 | April 2024		
Actual date of submission	PM 22		
Lead beneficiary: UNIVBRIS	Work package: WP6	Nature: REPORT	Dissemination level: PU
Responsible scientist	M. Rigby		
Contributors	E. Saboya, P. Pickers, A, van der Woude, W. Peters		
Internal reviewers	-		
Version: 1			

Horizon Europe Cluster 5: Climate, energy and mobility

"This project has received funding from the European Union's Horizon Europe Research and Innovation programme under HORIZON-CL5-2022-D1-02 Grant Agreement No 101081430 - PARIS".

M24 – Inverse estimates of fossil fuel CO_2 emission

Table of contents

1. Changes with respect to the DoA (Description of the Action)

This milestone report is delayed by approximately 4 months due to unforeseen technical challenges associated with inverse model development, staff changes and staff absence.

2. Dissemination and uptake

Milestone M24 is the preparation of preliminary fossil fuel CO_2 emissions estimates through inverse modelling for the PARIS CO_2 focus countries, the UK and Netherlands. When they reach maturity, these inverse estimates will underpin contributions to future draft National Inventory Report Annexes, to be presented to the UK and Netherlands inventory compilers.

3. Short summary of results

The evaluation of fossil fuel CO_2 emissions using atmospheric observations is extremely challenging because the observed variations in CO_2 mole fraction measurements (e.g., Fig. 1) are strongly influenced by biosphere fluxes. Here, we report on the current state of PARIS fossil fuel CO_2 emissions evaluation in the UK and Netherlands using simultaneous atmospheric measurements of CO_2 and O_2, and using a high-resolution regional CO_2 inversion system. Our preliminary results demonstrate the challenging nature of this problem. Given the current uncertainties in these approaches, no discrepancies in the fossil fuel CO_2 emissions inventories can be confidently derived at present. Improvements are expected in the next two years with the expanded CO_2/O_2 measurement network that PARIS and other projects will provide, along with continuing improvements in inverse modelling systems for the quantification of $ffCO_2$ from atmospheric measurements.

4. Evidence of accomplishment

A brief summary of our preliminary results is presented below. Section 4.1 details a scoping study on the use of $ffCO_2$ derived from atmospheric CO_2 and O_2 measurements combined with the UK Met Office NAME atmospheric chemical transport model, and Section 4.2 shows preliminary results using the CarbonTracker-Europe system atmospheric transport model.

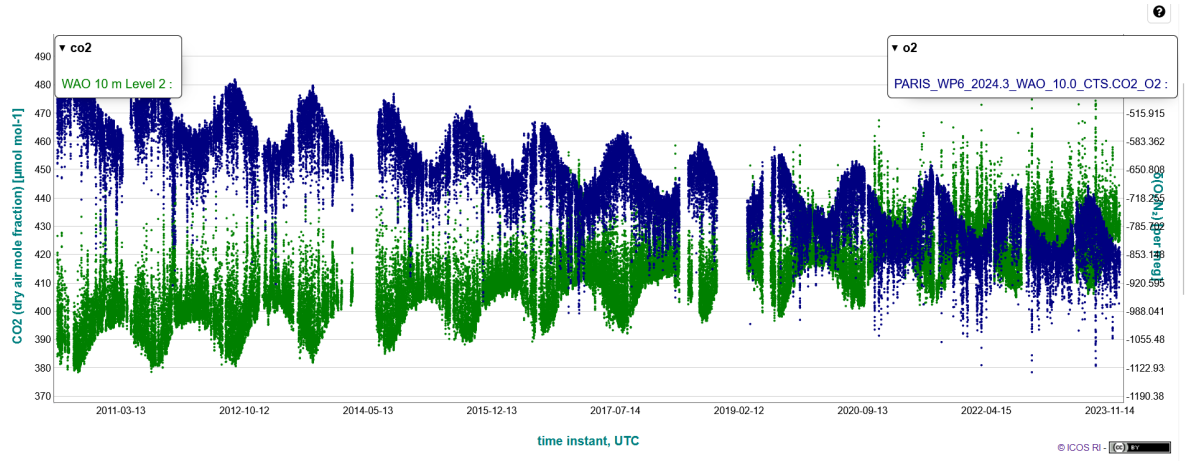

Fig. 1: Atmospheric O_2 and CO_2 data from Weybourne Atmospheric Observatory on the ICOS Carbon Portal website (see PARIS Milestone 21 report, Pickers et al., 2024, https://horizoneurope-paris.eu/wp-content/uploads/sites/914/2024/05/MS21-Blind-inverse-modelling-experiment-protocol-published-final.pdf).

4.1 Preliminary inverse estimates of fossil fuel CO_2 using atmospheric potential oxygen

Disentangling the anthropogenic CO_2 contribution to overall CO_2 variability is challenging. On short timescales and regional scales, above- or below-baseline mole fraction deviations due to terrestrial biosphere CO_2 mole fractions are often substantially larger than those due to fossil fuels. Concurrent atmospheric measurements of oxygen (O_2) and CO_2 can be combined into the tracer 'Atmospheric Potential Oxygen' (APO) according to $APO = O_2 + 1.1 \times CO_2$, where 1.1 denotes the mean O_2:CO_2 ratio of exchange between the terrestrial biosphere and the atmosphere (Stephens et al., 1998; Severinghaus, 1995). APO is therefore, by design, invariant to terrestrial biospheric influences. APO has previously been used as a tracer for ocean carbon cycle processes, which occur predominantly on seasonal and longer-term timescales, but regional fossil fuel CO_2 ($ffCO_2$) influences can also be estimated in APO by subtracting a suitable baseline that incorporates these seasonal and long-term oceanic APO variations (Pickers et al., 2022), according to:

$$ffCO_2[APO] = (APO - APO_{BL})/R_{APO} \quad (1)$$

where APO_{BL} is the 'baseline' APO (i.e., APO that represents the well-mixed background conditions at that latitude without any local influences) and R_{APO} is the molar ratio (R) of APO:CO_2 for fossil fuel emissions.

Here, atmospheric $ffCO_2$ mole fractions are derived from CO_2 and O_2 observations combined into APO, made at the Weybourne Atmospheric Observatory on the east coast of England. These APO-based $ffCO_2$ mole are then used to evaluate simulated $ffCO_2$ mole fractions at Weybourne using fluxes from the high-resolution CarbonTracker Europe (CTE-HR) product.

4.1.1 Atmospheric measurement approach for deriving $ffCO_2$

Concurrent atmospheric O_2 and CO_2 measurements have been routinely made at the coastal Weybourne Atmospheric Observatory (WAO) in the east England (e.g. Adcock et al., 2023) since May 2010, and at the Heathfield Tall Tower in Sussex from June 2021 – Nov 2022, and from Jan 2024 onwards. These atmospheric O_2 and CO_2 measurements can be combined into APO as defined in section 4.1 above. The APO-derived $ffCO_2$ mole fractions for WAO are shown in Fig. 2 for the year 2022.

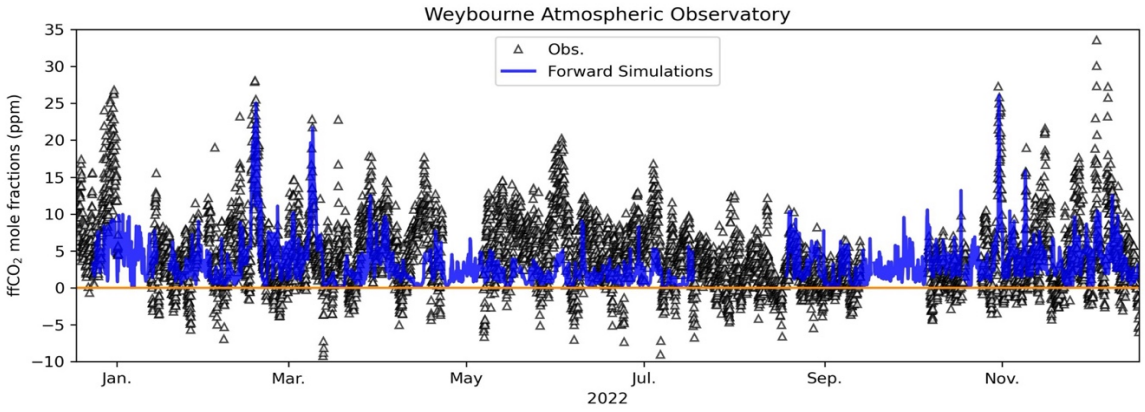

Fig. 12: Atmospheric $ffCO_2$ mole fraction estimates at WAO from APO observations (black) and simulated using CTE-HR fossil fluxes and NAME footprints (blue) for all hours.

The APO-based $ffCO_2$ estimates shown in this report are currently preliminary and do not currently include a full quantification of uncertainties. Uncertainties in the derived $ffCO_2$ arise from three sources: uncertainties from the CO_2 and O_2 measurements, uncertainties from determination of the baseline, and uncertainties from R_{APO}. The baseline and R_{APO} uncertainties usually dominate the overall $ffCO_2$ uncertainty more than the measurement uncertainties. At present, the baseline has been determined using a statistical fitting technique known as 'RFbaseline' (Ruckstuhl et al., 2012) with a smoothing window value of 0.02, which for hourly data is roughly equivalent to 1 week. For R_{APO}, a constant value of 0.4 has been used according to Chawner et al., (2024). Incorrect determination of the baseline and/or the mean R_{APO} value can lead to biases in the calculated $ffCO_2$, thus it will be important to refine these terms in future work and to report $ffCO_2$ uncertainties.

4.1.2 Simulating a priori $ffCO_2$ estimates

Hourly fossil fuel flux fields from the 2022 High Resolution Carbon-Tracker Europe product (CTE-HR; Van der Woude et al., 2023) form the *a priori* flux estimates of our simulation and inversion. CTE-HR fossil fuel fluxes have a 0.2° x 0.1° spatial resolution spanning 15 °W to 35 °E and 33 °N to 72 °N, which are "re-gridded" to match the spatial resolution of the chemical transport model using a mass-conservative approach. Fossil fuel fluxes are produced using a dynamic anthropogenic emissions model that is driven by economic activity and energy-use statistics, and meteorology from the European Centre for Medium-range Weather Forecasting (ECMWF) Reanalysis 5th generation (ERA5) meteorology (Hersbach et al., 2020). Further details of CTE-HR fluxes are described in Van Der Woude et al., 2023.

The relationship between surface emissions and atmospheric mole fractions measured at WAO was quantified using the UK Met Office Lagrangian dispersion model, NAME (Numerical Atmospheric dispersion Modelling Environment; Jones et al., 2007). "Footprints" of surface emissions sensitivities were calculated from particle back-trajectory ensembles. Each grid cell of the footprint describes the influence of emissions from that grid cell on the measured mole fractions at the measurement site at a certain time.

Hourly footprints were calculated as described in White et al. (2019) with a ~25x25 km^2 (0.352°x0.234°) spatial resolution over a model domain spanning approximately 98 °W to 40 °E and 11 °N to 79 °N using 30-day air-histories. The first 24 hours of the air-history are time-disaggregated to account for rapid flux variations in CO_2 with the remaining 29 days of the air-history being time-integrated. This approach for modelling the transport of CO_2 fluxes is further described in White et al. (2019) and Chawner et al. (2024). Meteorological fields from the Met Office Unified Model (UM) underpin the footprints with hourly, high-resolution (0.0135° x 0.0135°, 57 vertical levels up to ~12 km) UKV meteorological fields used for over the British Isles and three-hourly UM (0.1406° X 0.0938° with 59 vertical levels up to ~30 km) global meteorological fields for the rest of the model domain.

Footprints were combined with the fossil fuel CTE-HR flux fields to simulate atmospheric $ffCO_2$ mole fractions at WAO (Fig. 2).

4.1.3 Inverse modelling approach for deriving $ffCO_2$ emissions

Inverse models are often used to derive emissions estimates from atmospheric trace gas measurements through Bayesian inference. This measurement-informed (top-down) approach is typically independent of bottom-up emissions inventory totals and trends that are reported to the UNFCCC (United Nations Framework Convention on Climate Change).

Top-down approaches can therefore be used to evaluate emissions inventory estimates (e.g. Saboya et al., 2024; Manning et al., 2011), and identify where bottom-up methodologies may need refining.

Bayes' theorem often underlies the framework of atmospheric trace gas inverse methods. Here, a simple Bayesian inverse method is used to derive a scaling of the simulated ffCO2 mole fraction, $\boldsymbol{x}$, by comparing the NAME simulation to atmospheric trace gas observations, $\boldsymbol{y}$, starting from an a priori estimate $\boldsymbol{x_a}$, equal to 1. Here, the NAME footprints are combined with the CTE-HR fluxes to define the forward model, **K**. Covariance matrixes $\boldsymbol{S_O}$ *and* $\boldsymbol{S_a}$ capture model-observation uncertainties and a priori uncertainties, respectively. Uncertainties are assumed to be uncorrelated such that $\boldsymbol{S_O}$ *and* $\boldsymbol{S_a}$ are diagonal. When Gaussian error distributions are assumed, the *a posteriori* probability density function, $\boldsymbol{P(x|y)}$, can be written as:

$$P(\boldsymbol{x}|\boldsymbol{y}) \propto \exp\left(-\frac{1}{2}(\boldsymbol{y}-\boldsymbol{Kx})^T\boldsymbol{S_O^{-1}}(\boldsymbol{y}-\boldsymbol{Kx}) - \frac{1}{2}(\boldsymbol{x_a}-\boldsymbol{x})^T\boldsymbol{S_a^{-1}}(\boldsymbol{x_a}-\boldsymbol{x})\right) \quad (2)$$

The maximum a posteriori solution to (2) is:

$$\hat{\boldsymbol{x}} = \boldsymbol{x_a} + \hat{\boldsymbol{S}}\boldsymbol{K^T}\boldsymbol{S_o^{-1}}(\boldsymbol{y}-\boldsymbol{Kx_a}) \quad (3)$$

where $\hat{\boldsymbol{S}}$, is the a posteriori covariance matrix,

$$\hat{\boldsymbol{S}} = \left(\boldsymbol{K^T}\boldsymbol{S_O^{-1}}\boldsymbol{K} + \boldsymbol{S_a^{-1}}\right)^{-1} \quad (4)$$

Diagonal model-observation $ffCO_2$ uncertainties of 10 ppm were estimated, based on the largest below-baseline derviation of the observationally derived $ffCO_2$ estimates, and *a priori* uncertainties of 100% are imposed. Data are filtered to retain observations made during the daytime hours (10.00-14.00 LT; Fig. 3). During the daytime, the mixed layer of the planetary boundary layer tends to be deeper and thus air samples are more representative of the region and better captured in the atmospheric transport model.

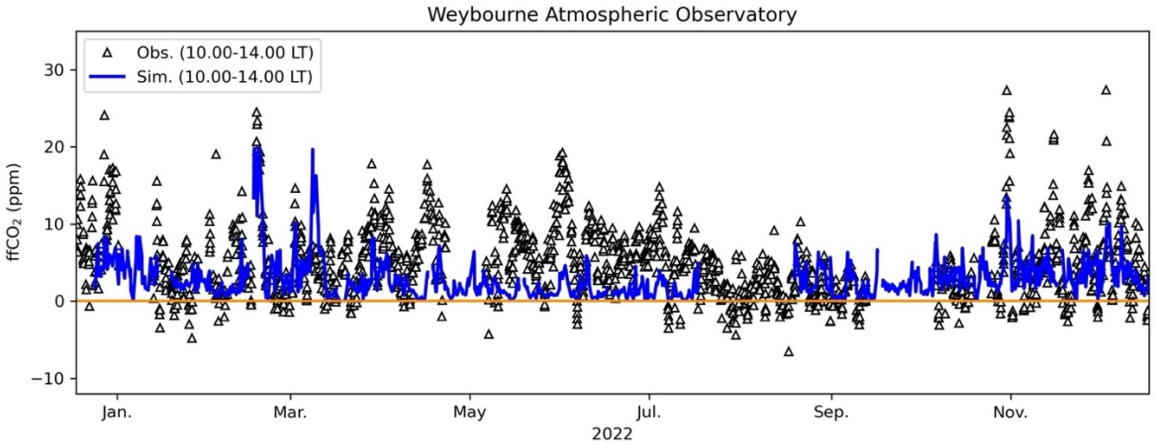

Fig. 23: Atmospheric $ffCO_2$ mole fraction estimates at WAO from APO observations (black) and simulated using CTE-HR fossil fluxes and NAME footprints (blue) filtered to retain data between 10.00-14.00 LT.

4.1.4 $ffCO_2$ model-data comparison and inverse estimates

4.1.4.1 APO-derived $ffCO_2$ mole fractions

Mean WAO $ffCO_2$ mole fractions of 4.7±4.7 (1σ) ppm are derived from using the APO approach for the year 2022. However, in this approach ~10% of $ffCO_2$ mole fractions have negative values, as all $ffCO_2$ is calculated relative to the APO baseline fit with some APO values remaining above the baseline (whereas $ffCO_2$ signals manifest as below-baseline excursions). Once $ffCO_2$ uncertainties have been quantified, we expect that a significantly lower percentage of the dataset will result in negative $ffCO_2$ values outside of the uncertainty ranges. In addition, using a baseline in future that is more consistent with the model-produced $ffCO_2$ will help to eliminate baseline-related biases between the observation and model derived $ffCO_2$ estimates. Mean daytime $ffCO_2$ values of 5.9±4.9 (1σ) ppm are calculated between January and March 2022, whereas between October and December 2022, daytime $ffCO_2$ had a mean value of 4.8±5.3 (1σ) ppm. Higher $ffCO_2$ values are expected during the winter months when energy demands from residential heating are typically higher compared to the summertime.

4.1.4.2 Simulated $ffCO_2$ mole fractions

Hourly $ffCO_2$ mole fractions were simulated at WAO for the year 2022 using CTE-HR fossil fuel fluxes combined with the atmospheric transport model NAME (Section 2.2). The mean simulated $ffCO_2$ mole fraction is 3.1±2.8 (1σ) ppm for the year 2022 when considering data from all hours. However, the mean $ffCO_2$ mole fraction is 2.9±2.7 (1σ) ppm when considering only daytime data from across 2022.

Similar to the APO-derived $ffCO_2$ estimates, when considering simulated $ffCO_2$ mole fractions from January to March and October to December, the mean daytime values are higher than the annual $ffCO_2$ means with a value of 4.1±3.9 (1σ) ppm and 4.0±2.3 (1σ) ppm, respectively.

4.1.4.3 Inverse Modelling Results

Monthly inversions were performed to infer *a posteriori* $ffCO_2$ mole fraction estimates at WAO using daytime data (Fig. 4). We limited the scope of our inversions to January-March and October-December 2022. The results from these inversions are shown in Fig. 4.

Across the January-March period an average *a priori* scale factor of 1.43 (0.14-2.97; 68% confidence interval) was inferred. This non-statistically significant scaling indicates that $ffCO_2$ mole fractions are ~43% higher than produced in the simulations. For October-December an average (non-statistically significant) *a posteriori* scale factor of 1.83 (0.15-3.51; 68% confidence interval) was inferred indicating poorer agreement between the APO-derived and simulated $ffCO_2$ mole fractions during this period than for January-March. There are, however, instances when the *a posteriori* solutions do not capture certain large $ffCO_2$ pollution events (e.g. in mid-February and in late November).

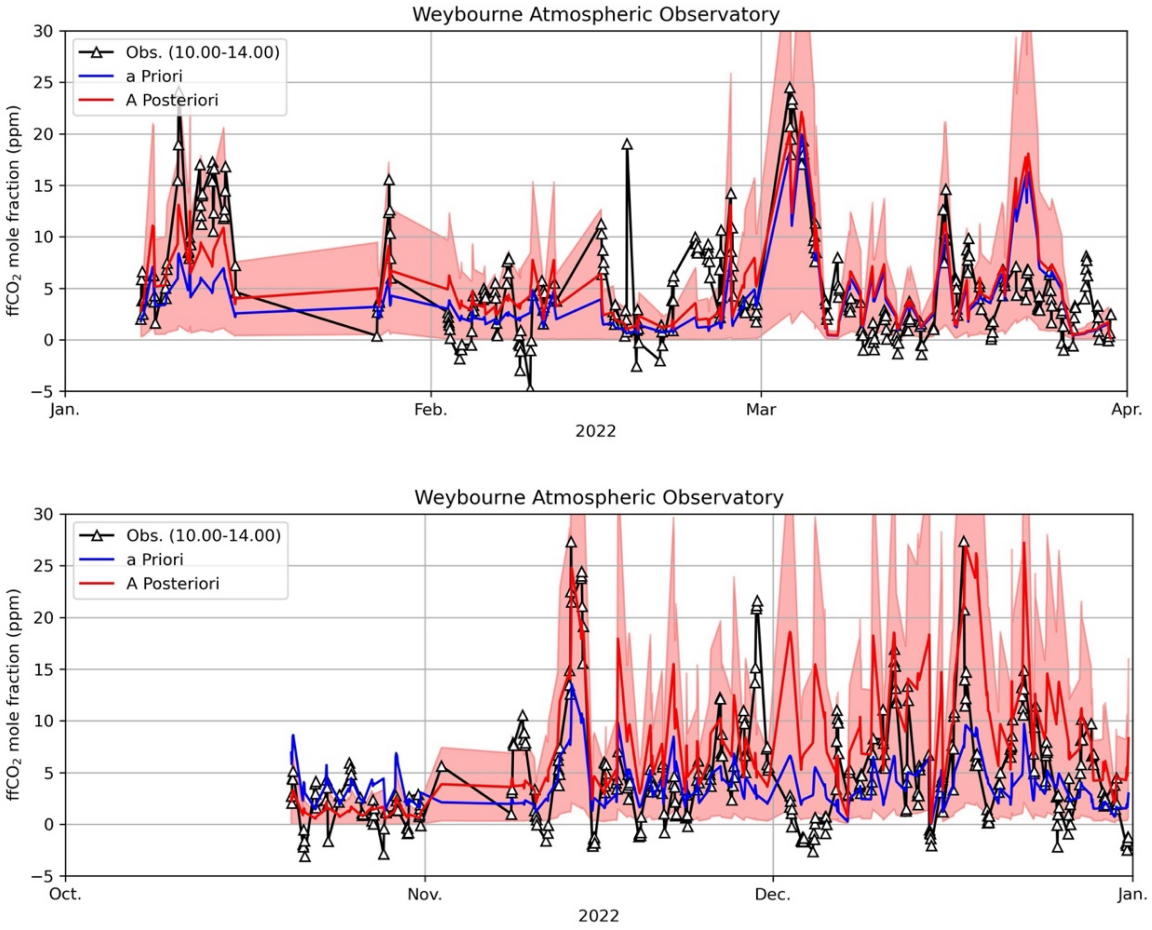

Fig. 34: Comparison of model and observation-based $ffCO_2$ mole fractions at WAO between 10.00-14.00. APO-derived ffCO2 are shown in black and simulated values (a priori) are shown in blue. The inferred (a posteriori) solution is shown in red with the 1-sigma uncertainty range indicated by the red band.

4.1.5 Discussion

Our preliminary inversions indicate APO-derived $ffCO_2$ values are substantially higher than indicated by NAME simulations across 6 months of 2022. However, given the uncertainties, the derived scalings are not statistically significant, meaning that our results are statistically consistent with the bottom-up estimates. Furthermore, the APO-derived $ffCO_2$ values are preliminary and may change in future iterations following our refinement of the baseline and R_{APO} estimates. The presence of substantially below-background APO-derived ffCO2 indicates that the identification of background APO is likely to be a key area where improvements are needed. At present, the baseline used to calculate the APO-derived $ffCO_2$ is not necessarily consistent with the model-derived $ffCO_2$, which by definition will always have a baseline value of exactly 0. One potential way to overcome model versus observation baseline methodological differences is to examine the $ffCO_2$ gradients (i.e. differences) between WAO and the Heathfield Tall Tower (HFD). Another way would be to compare $ffCO_2$ between successive years, as again any baseline-related methodological differences should cancel out.

Through PARIS and the Horizon Europe CORSO project, two new APO measurement stations will be established in the Netherlands. Future versions of this study will incorporate these sites into the inversion framework as well as make use of APO data from HFD in Sussex, and will focus on the south-east of England and the Netherlands, the regions to which these data are most sensitive.

4.2 High-resolution regional CO_2 inverse modelling using CarbonTracker-Europe

Similar to the APO inversion described above, the CarbonTracker Europe high-resolution regional inverse system (CTE-HR-inv) uses Bayesian statistics to infer carbon fluxes. This system is based on CarbonTracker Europe (CTE, van der Laan-Luijkx, 2017) and its Lagrangian version, CTE-Lagrange (He et al., 2018) and uses the ensemble Kalman Filter to solve for regional carbon fluxes. On global scales, for which CTE is designed, fossil fuel emissions have a small uncertainty, about 5%, and the main uncertainty in the global carbon budget is in the ocean and biogenic fluxes. On the contrary, on the regional scale of CTE-HR-inv (shown in Fig. 5, fossil fuel emissions are more uncertain. This is because yearly, national fossil fuel use is quite well constrained, but spatio-temporal upscaling of these fluxes adds uncertainty. Over the domain (Fig. 5), the ocean plays a minor role. Therefore, we have chosen to optimise both fossil fuel emissions and biogenic fluxes in CTE-HR-inv.

Although the system is in principle similar to CTE-Lagrange (He et al., 2018), some key differences are present. Besides a code overhaul, from the R programming language to Python, we use both different prior assumptions and a different state vector. These are explained in more detail below.

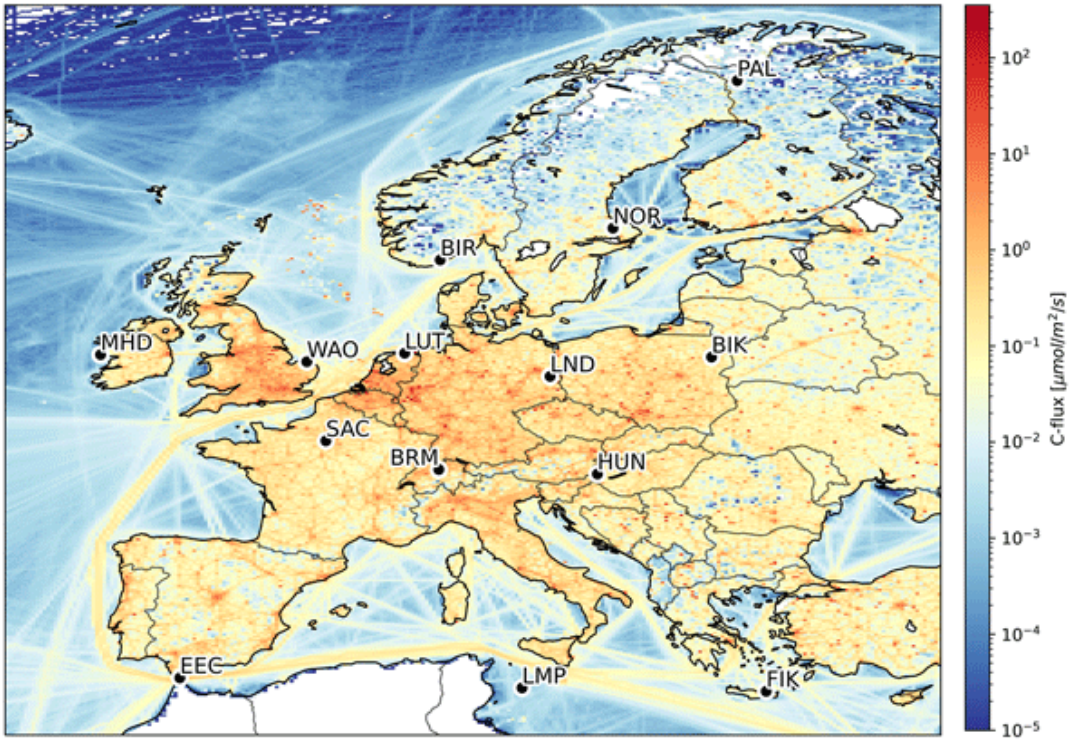

Fig. 45: *The European domain of CTE-HR-inv, with fossil fuel emissions for July 8, 2018 as example. Taken from van der Woude et al. (2023).*

4.2.1 Prior fluxes

For prior fluxes we use the high-resolution fluxes from CTE-HR (Van der Woude et al., 2023). CTE-HR provides hourly fossil fuel emissions, as well as oceanic and biogenic exchange at a resolution of 0.1x0.2 degree over Europe (See Fig. 5).

The fossil fuel emissions in CTE-HR are informed by open-source statistics, such as electricity generation and amount of fuel sold. With this information, the effect of carbon emissions by events such as the COVID-19 crisis, but also the reduction of electricity use during Christmas, are captured.

The biogenic exchange in CTE-HR is estimated by the biosphere model SiB4 (Haynes et al., 2020). SiB4 uses meteorology (taken from ERA5) to calculate carbon uptake by plants and exchange between different carbon pools. In CTE-HR, the 0.5x0.5 degree carbon fluxes from SiB4 are upscaled to the 0.1x0.2 degree resolution by applying a high-resolution land-use type mask. The oceanic fluxes are taken from an optimised ocean product and upscaled based on temperature and wind-speed.

4.2.2 Optimisation settings

For the biosphere fluxes, we expect the errors in SiB4 to be land-use type specific. Additionally, we restart SiB4 from a steady-state, meaning that there is no age included. Therefore, we also expect errors in SiB4 to be forest age-related. Finally, different countries have different management regimes, resulting in different forest structures, which are not present in SiB4. We thus expect biosphere fluxes in different countries to behave differently. Based on these considerations, we optimise the net ecosystem exchange (NEE) per country per age-class. On each of these 503 parameters, we put an uncertainty of 2 umol/m^2/s. To limit the degrees of freedom, we apply a decay in temporal correlation with a half-time of 4 days. This synoptic time scale reflects the time scales in which weather patterns, and thus short-term variability in the biosphere, changes. We have chosen to optimise an additive scaling factor on NEE, as prior NEE can be both positive and negative, depending on the season, and is very small in the shoulder seasons. A very small NEE signal requires a very large multiplicative scaling factor. These potential issues are resolved with the additive scaling factor.

Errors in total anthropogenic emissions stem mainly from errors in reporting and the use of the activity data. We therefore assume that these errors are unique for each of the 43 countries in the domain. Contrary to NEE, of which the sign can flip depending on the season, anthropogenic emissions are always positive. Therefore, we have chosen to use multiplicative scaling for the anthropogenic emissions. This choice also results in smaller uncertainties at times when total prior emissions are smaller. The errors in the reporting and activity data that inform the anthropogenic emissions are slowly varying parameters, such as energy efficiency of the industry. We expect these parameters to change only slowly over time. We therefore apply a large temporal correlation, with a half-time of two weeks. We put an uncertainty of 20% on the anthropogenic emissions.

We take the background as the optimised 3D mole fractions from CTE2022. Although these mole fractions are optimally consistent with the atmospheric growth rate, they are not a perfect representation of the CO_2 distribution. We optimise the background additively over 8 regions, based on the wind-sector (NNE, NE, SE, SSE, SSW, SW, NW, NNW). We expect the

errors in the background to vary over synoptic timescales and have thus chosen a temporal correlation with a half-time of 6 days and an uncertainty of 0.3 ppm.

4.2.3 Preliminary results

We find that the European biosphere in 2021 has been a sink of about 300 TgC/y. We note that this is consistent with estimates by Scholze et al., (2019), Monteil et al., (2020) and Peters et al., (2010). Nevertheless, a significant uncertainty of 90 TgC/y exists in the biogenic European carbon fluxes.

Simultaneously, we find that total fossil fuel emissions in the Euro-pean domain are about 1200 TgC/y. This is consistent with inventories, although a direct comparison to inventories is difficult due to different processes included in different inventories. For the anthropogenic emissions, smaller uncertainties of 11TgC/y (1%) remain after optimisation with atmospheric observations of CO_2.

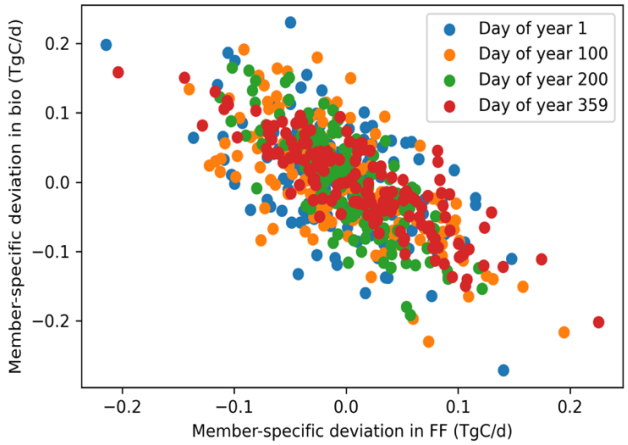

Fig. 56: *member-specific deviations for both fossil fuel (x-axis) and biogenic (y-axis) fluxes over Germany for specific days of 2021. The negative correlation indicates that a member with relatively high fossil fuel emissions compensates with lower (more negative) biogenic fluxes.*

Even though the our most likely estimate of both the total biogenic sink of CO_2 and the total fossil fuel emitted in Europe seem to be in accordance with previous findings, we cannot distinguish them in our inversions, based on only atmospheric CO_2 observations. This can be seen in Fig. 6, in which the flux deviations in both bio-genic and fossil fuels for individual ensemble members (N=150) is shown. Fig. 6 shows a clear negative correlation. This means that ensemble members with higher fossil fuel fluxes compensate this with lower biospheric fluxes. This effect is strongest for Germany, as most observation sites are in Germany.

4.3 Conclusion

The PARIS project, in collaboration with the Horizon Europe CORSO project, will establish a "mini-network" of four APO measurement sites in the south-east of the UK and the Netherlands. Here, we demonstrate our current capability using long-running measurements from Weybourne, the NAME chemical transport model and a simplified Bayesian inversion. Our preliminary results show some agreement between APO-ffCO_2 and simulated ffCO_2 mole fractions. However, the uncertainty in this approach is currently very large, and we cannot yet recommend a revision of inventory estimates.

We performed and analysed an atmospheric inversion with high-resolution European carbon dioxide fluxes. Although mean total fluxes of both anthropogenic and biogenic fluxes are consistent with other data sources, we cannot distinguish the separate fluxes from only atmospheric CO_2 mole fractions. This shows that, to constrain anthropogenic emissions from the atmosphere, also a better constraint on biogenic fluxes is required. This can may be achieved by using different tracers that are complementary to CO_2 in the inversion system, such as APO or radiocarbon.

4.4 References

Adcock, K. E., Pickers, P. A., Manning, A. C., Forster, G. L., Fleming, L. S., Barningham, T., Wilson, P. A., Kozlova, E. A., Hewitt, M., Etchells, A. J., & Macdonald, A. J. (2023). 12 years of continuous atmospheric O2, CO2 and APO data from Weybourne Atmospheric Observatory in the United Kingdom. *Earth System Science Data*, *15*(11). https://doi.org/10.5194/essd-15-5183-2023

Battle, M., Fletcher, S. M., Bender, M. L., Keeling, R. F., Manning, A. C., Gruber, N., Tans, P. P., Hendricks, M. B., Ho, D. T., Simonds, C., Mika, R., & Paplawsky, B. (2006). Atmospheric potential oxygen: New observations and their implications for some atmospheric and oceanic models. *Global Biogeochemical Cycles*, *20*(1). https://doi.org/10.1029/2005GB002534

Chawner, H., Saboya, E., Adcock, K. E., Arnold, T., Artioli, Y., Dylag, C., Forster, G. L., Ganesan, A., Graven, H., Lessin, G., Levy, P., Luijkx, I. T., Manning, A., Pickers, P. A., Rennick, C., Rödenbeck, C., & Rigby, M. (2024). Atmospheric oxygen as a tracer for fossil fuel carbon dioxide: a sensitivity study in the UK. *Atmospheric Chemistry and Physics*, *24*(7), 4231–4252. https://doi.org/10.5194/acp-24-4231-2024

He, W., Velde, I. R. Van Der, Andrews, A. E., Sweeney, C., Miller, J., Tans, P., Laan-Luijkx, I. T. Van Der, Nehrkorn, T., Mountain, M., Ju, W., Peters, W., Chen, H., Van Der Velde, I. R., Andrews, A. E., Sweeney, C., Miller, J., Tans, P., Van Der Laan-Luijkx, I. T., Nehrkorn, T., … Chen, H. (2018). CTDAS-Lagrange v1.0: A high-resolution data assimilation system for regional carbon dioxide observations. Geoscientific Model Development, 11(8), 3515–3536. https://doi.org/10.5194/gmd-11-3515-2018

Hersbach, H. , Bell, B. , Berrisford, P. , Biavati, G. , Horányi, A. , Muñoz Sabater, J. , Nicolas, J., Peubey, C. , Radu, R. , Rozum, I. , Schepers, D. , Simmons, A. , Soci, C. , Dee, D. , & Thépaut, J.-N. (2023). ERA5 hourly data on single levels from 1940 to present. Copernicus Climate Change Service (C3S) Climate Data Store (CDS), DOI: 10.24381/cds.adbb2d47 (Accessed on 06-Sep-2023). *Ecmwf*, *147*.

Jones, A., Thomson, D., Hort, M., & Devenish, B. (2007). The U.K. Met Office's Next-Generation Atmospheric Dispersion Model, NAME III. In *Air Pollution Modeling and Its Application XVII* (pp. 580–589). Springer US. https://doi.org/10.1007/978-0-387-68854-1_62

Keeling, R. F. (1988). Measuring correlations between atmospheric oxygen and carbon dioxide mole fractions: A preliminary study in urban air. *Journal of Atmospheric Chemistry*, *7*(2), 153–176. https://doi.org/10.1007/BF00048044

Van der Laan-Luijkx, I. T., der Velde, I. R. Van, Veen, E. Van Der, Tsuruta, A., Stanislawska, K., Babenhauserheide, A., Zhang, H. F., Liu, Y., He, W., Chen, H., Masarie, K. A., Krol, M. C., Peters, W., Van der Laan-Luijkx, I. T., Van der Velde, I. R., Van Der Veen, E., Tsuruta, A., Stanislawska, K., Babenhauserheide, A., … Peters, W. (2017). The CarbonTracker Data Assimilation Shell (CTDAS) v1.0: Implementation and global carbon balance 2001-2015. Geoscientific Model Development, 10(7), 2785–2800. https://doi.org/10.5194/gmd-10-2785-2017

Manning, A. J., O'Doherty, S., Jones, A. R., Simmonds, P. G., & Derwent, R. G. (2011). Estimating UK methane and nitrous oxide emissions from 1990 to 2007 using an inversion modeling approach. *Journal of Geophysical Research Atmospheres*, *116*(2), 1–19. https://doi.org/10.1029/2010JD014763

Pickers, P. A., Manning, A. C., Quéré, C. le, Forster, G. L., Luijkx, I. T., Gerbig, C., Fleming, L. S., & Sturges, W. T. (2022). Novel quantification of regional fossil fuel CO2 reductions during COVID-19 lockdowns using atmospheric oxygen measurements. *Science Advances*, *8*(16). https://doi.org/10.1126/sciadv.abl9250

Ruckstuhl, A.F., S. Henne, S. Reimann, M. Steinbacher, M. K. Vollmer, S. O'Doherty, B. Buchmann, C. Hueglin, Robust extraction of baseline signal of atmospheric trace species using local regression. *Atmospheric Measurement Techniques,* 5, 2613–2624 (2012). https://doi.org/10.5194/amt-5-2613-2012.

Saboya, E., Manning, A. J., Levy, P., Stanley, K. M., Pitt, J., Young, D., Say, D., Grant, A., Arnold, T., Rennick, C., Tomlinson, S. J., Carnell, E. J., Artioli, Y., Stavart, A., Spain, T. G., O'Doherty, S., Rigby, M., & Ganesan, A. L. (2024). Combining Top-Down and Bottom-Up Approaches to Evaluate Recent Trends and Seasonal Patterns in UK N_2O Emissions. *Journal of Geophysical Research: Atmospheres*, *129*(14). https://doi.org/10.1029/2024JD040785

Severinghaus, J.P. (1995). Studies of the terrestrial O2 and carbon cycles in sand dunes gases and biosphere. Thesis, Columbia University.

Stephens, B. B., Keeling, R. F., Heimann, M., Six, K. D., Murnane, R., & Caldeira, K. (1998). Testing global ocean carbon cycle models using measurements of atmospheric O2 and CO2 concentration. *Global Biogeochemical Cycles*, *12*(2). https://doi.org/10.1029/97GB03500

van der Woude, A. M., de Kok, R., Smith, N., Luijkx, I. T., Botía, S., Karstens, U., Kooijmans, L. M. J., Koren, G., Meijer, H. A. J., Steeneveld, G. J., Storm, I., Super, I., Scheeren, H. A., Vermeulen, A., & Peters, W. (2023). Near-real-time CO2fluxes from CarbonTracker Europe for high-resolution atmospheric modeling. *Earth System Science Data*, *15*(2). https://doi.org/10.5194/essd-15-579-2023

White, E. D., Rigby, M., Lunt, M. F., Luke Smallman, T., Comyn-Platt, E., Manning, A. J., Ganesan, A. L., O'Doherty, S., Stavert, A. R., Stanley, K., Williams, M., Levy, P., Ramonet, M., Forster, G. L., Manning, A. C., & Palmer, P. I. (2019). Quantifying the UK's carbon dioxide flux: An atmospheric inverse modelling approach using a regional measurement network. *Atmospheric Chemistry and Physics*, *19*(7). https://doi.org/10.5194/acp-19-4345-2019

van der Woude, A. M., de Kok, R., Smith, N., Luijkx, I. T., Botía, S., Karstens, U., Kooijmans, L. M. J., Koren, G., Meijer, H. A. J., Steeneveld, G.-J., Storm, I., Super, I., Scheeren, H. A., Vermeulen, A., Peters, W., Van der Woude, A. M., de Kok, R., Smith, N., Luijkx, I. T., … Peters, W. (2023). Near-real-time CO 2 fluxes from CarbonTracker Europe for high-resolution atmospheric modeling. *Earth System Science Data*, *15*(2), 579–605. https://doi.org/10.5194/essd-15-579-2023

5. History of the document

Version	Author(s)	Date	Changes
V 1.0	M. Rigby, E. Saboya	17/06/2024	New document
	S. Walter	14 October 2024	feedback
	M. Rigby, E. Saboya	17 October 2024	Final version
	S. Walter	17 October 2024	Final formatting